J. Am. Chem. Soc. 1983, 105, 4310-4318

# Reactivity Properties of Single $MoFe_3S_4$ Cubane-Type Clusters: Synthesis, Structure, and Ligand Substitution Reactions of $[MoFe_3S_4Cl_3(3,6\text{-}(C_3H_5)_2C_6H_2O_2)(THF)]^{2-}$

**R. E. Palermo and R. H. Holm***

*Contribution from the Department of Chemistry, Harvard University, Cambridge, Massachusetts 02138.* *Received December 2, 1982*

**Abstract:** Reaction of the doubly-bridged double-cubane cluster $[Mo_2Fe_6S_8(SEt)_6(al_2cat)_2]^{4-}$ ($al_2cat$ = 3,6-diallylcatecholate) with 6 equiv of acetyl chloride in acetonitrile afforded, after recrystallization from acetone/THF, the single-cubane compound $(Et_4N)_2[MoFe_3S_4Cl_3(al_2cat)(THF)]\cdot 0.5CH_3COCH_3$. The acetone-free compound crystallizes from *n*-butyronitrile/THF in monoclinic space group $C2/c$ with $a$ = 23.829 (5) Å, $b$ = 11.452 (3) Å, $c$ = 16.870 (3) Å, $\beta$ = 106.15 (2)°, and $Z$ = 4. With use of 2451 unique data ($F_o^2 > 3\sigma(F_o^2)$) the structure was refined to $R$ ($R_w$) = 3.88% (3.94%). The cluster $[MoFe_3S_4Cl_3(al_2cat)(THF)]^{2-}$ (**1**) has a cubane-type $[MoFe_3(\mu_3\text{-}S)_4]^{3+}$ core with tetrahedral Fe atoms terminally coordinated by chloride and a Mo atom whose coordination external to the core is completed by a catecholate chelate ring and a THF molecule (Mo–O = 2.352 (6) Å). An imposed mirror plane bisects the core and the chelate ring, resulting in cluster $C_s$ symmetry and two types of Fe sites ($2m'' + m'$). In solution the cluster solvates $[MoFe_3S_4Cl_3(al_2cat)(solv)]^{2-}$ (solv = MeCN (**2**), $Me_2SO$ (**3**)) are formed. These are fluxional owing to rapid exchange of bound and bulk solvent and are substitutionally labile at the Fe and/or Mo sites toward the ligands L = $RS^-$ (R = Ph, $p\text{-}CF_3C_6H_4$), $PEt_3$, and $CN^-$ present in stoichiometric amounts. All clusters exhibit isotropically shifted $^1H/^{19}F$ NMR spectra that are extremely sensitive to cluster structure. When Mo–L binding is nonlabile, the clusters are stereochemically rigid and all possible reaction products are detectable. From analysis of the NMR spectra it is shown that **2** reacts with 1–3 equiv of $RS^-$ preferentially at the Fe sites, forming $[MoFe_3S_4(SR)_{3-n}Cl_n(al_2cat)(MeCN)]^{2-}$ prior to development of the fully substituted Mo–SR cluster $[MoFe_3S_4(SR)_4(al_2cat)]^{3-}$ with a fourth equivalent of thiolate. In $Me_2SO$ the latter cluster is not formed. With 1 equiv of $PEt_3$ or $CN^-$ reaction of **2** occurs exclusively at the Mo site; no reaction with additional phosphine was observed. Reaction of the Mo–$PEt_3$ and Mo–CN clusters with 1–3 equiv of $RS^-$ and $CN^-$, respectively, generated the five possible clusters, including two diastereomeric pairs, all of which are nonfluxional. In $[MoFe_3S_4(SPh)_3(al_2cat)L)]^{2-,3-}$ the order of binding affinity at the Mo site is L = $RS^- < PEt_3 < CN^-$. This investigation provides the first information on the reactivity properties of substitutionally labile Mo and Fe atoms in a common cluster, **2** or **3**, having the same spin state ($S$ = $^3/_2$) as, and coordination sites resembling those in, the FeMo-cofactor of nitrogenase. Several apparent and possible reactivity parallels between the native and synthetic clusters are noted.

In the course of our more recent development of the chemistry of $MoFe_3S_4$ cubane-type clusters,[1-10] certain results of which have been summarized,[1] the synthesis and structures of the doubly-bridged double-cubanes **1** have been demonstrated.[2,6] It has further been shown that **1** undergoes the bridge cleavage reaction (eq 1) in coordinating solvents at ambient temperature to afford the solvated clusters **2**,[6] which could be trapped and isolated in the ligated forms **3** as crystalline $Et_4N^+$ salts by reaction 2.[4,8] Definitive evidence for the existence of single cubanes was obtained from the X-ray structure of one cluster **3**, $[MoFe_3S_4(S\text{-}p\text{-}C_6H_4Cl)_4(al_2cat)]^{3-}$ [4,8] ($al_2cat$ = 3,6-diallylcatecholate). The clusters **2** and others with the $[MoFe_3S_4]^{3+}$ core oxidation level exhibit certain similarities to the native clusters present in FeMo proteins and the FeMo-cofactor (FeMo-co) of nitrogenase that are relevant to the present investigation. More detailed comparisons are available elsewhere.[1,10] (i) Mo and Fe atoms are present in sulfide-rich coordination sites; on the basis of Mo[11-13] and Fe[14] EXAFS criteria the extent of resemblance of sites appears to be more pronounced for the Mo coordination unit, which in the native cluster also contains two to three low Z (O, N) donor atoms. (ii) Both types of clusters have $S$ = $^3/_2$ ground states;[4-7,10] these afford large isotropic shifts in $^1H$ and $^{19}F$ NMR spectra that appear to be largely contact in origin.[4-8] (iii) There is a similarity (not necessarily an identity) in Fe mean oxidation states, from

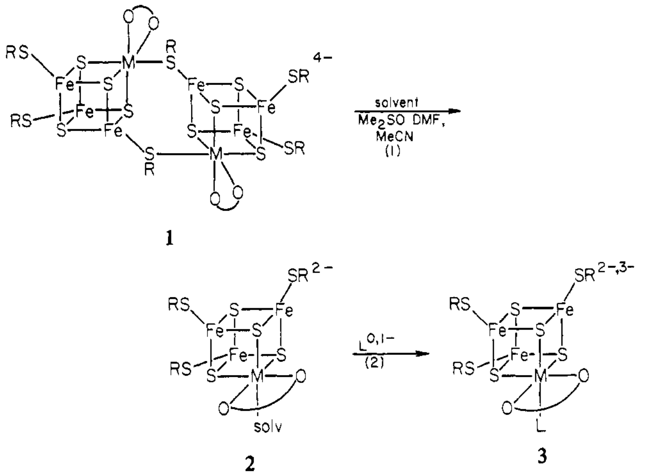

L = $RS^-$, $CN^-$, $RO^-$, $PR_3$

---

[1] Holm, R. H. *Chem. Soc. Rev.* **1981**, *10*, 455.

[2] Armstrong, W. H.; Holm, R. H. *J. Am. Chem. Soc.* **1981**, *103*, 6246.

[3] Palermo, R. E.; Power, P. P.; Holm, R. H. *Inorg. Chem.* **1982**, *21*, 173.

[4] Armstrong, W. H.; Mascharak, P. K.; Holm, R. H. *Inorg. Chem.* **1982**, *21*, 1699.

[5] Christou, G.; Mascharak, P. K.; Armstrong, W. H.; Papaefthymiou, G. C.; Frankel, R. B.; Holm, R. H. *J. Am. Chem. Soc.* **1982**, *104*, 2820.

[6] Armstrong, W. H.; Mascharak, P. K.; Holm, R. H. *J. Am. Chem. Soc.* **1982**, *104*, 4373.

[7] Mascharak, P. K.; Smith, M. C.; Armstrong, W. H.; Burgess, B. K.; Holm, R. H. *Proc. Natl. Acad. Sci. U.S.A.* **1982**, *79*, 7056.

[8] Mascharak, P. K.; Armstrong, W. H.; Mizobe, Y.; Holm, R. H. *J. Am. Chem. Soc.* **1983**, *105*, 475.

[9] Yamamura, T.; Christou, G.; Holm, R. H. *Inorg. Chem.* **1983**, *22*, 939.

[10] Mascharak, P. K.; Papaefthymiou, G. C.; Armstrong, W. H.; Foner, S.; Frankel, R. B.; Holm, R. H. *Inorg. Chem.*, in press.

[11] Cramer, S. P.; Hodgson, K. O.; Gillum, W. O.; Mortenson, L. E. *J. Am. Chem. Soc.* **1978**, *100*, 3398.

[12] Cramer, S. P.; Gillum, W. O.; Hodgson, K. O.; Mortenson, L. E.; Stiefel, E. I.; Chisnell, J. R.; Brill, W. J.; Shah, V. K. *J. Am. Chem. Soc.* **1978**, *100*, 3814.

[13] Burgess, B. K.; Yang, S.-S.; You, C.-B.; Li, J.-G.; Friesen, G. D.; Pan, W.-H.; Stiefel, E. I.; Newton, W. E.; Conradson, S. D.; Hodgson, K. O. In "Current Perspectives in Nitrogen Fixation"; Gibson, A. H., Newton, W. E., Eds.; Elsevier/North-Holland, Inc.: New York, 1981; pp 71–74.

[14] Antonio, M. R.; Teo, B.-K.; Orme-Johnson, W. H.; Nelson, M. J.; Groh, S. E.; Lindahl, P. A.; Kauzlarich, S. M.; Averill, B. A. *J. Am. Chem. Soc.* **1982**, *104*, 4703.

0002-7863/83/1505-4310$01.50/0

a comparison of isomer shifts of Fe atoms coupled to the $S = {}^3/_2$ spin system of FeMo-co with those of clusters having the core $[MoFe_3S_4]^{3+}$ oxidation level.[10,15] For the latter our isomer shift correlations lead to the probable (mean) oxidation numbers $Fe^{2.67+}$ + $Mo^{3+}$.[5,16]

Compositional differences between FeMo-co (atom ratios 6–8:9:1 Fe/S/Mo[1,17,18]) and synthetic clusters notwithstanding, the latter provide the best available vehicles for examination of reactivity properties of Mo and Fe atoms in sites structurally and electronically similar to those of the native cluster. A desirable goal is the development of nitrogenase substrate reduction systems based on reduced clusters, i.e., those with the $[MoFe_3S_4]^{2+}$ oxidation level. Single cubanes of this type have been generated in solution[8] and more recently have been isolated (unpublished results). Investigation of their reactivity properties is in progress. Here we describe the reactions of oxidized single cubanes with the pseudosubstrate ligands that are in general good $\sigma$ donors and/or $\pi$ acids. The set includes $PhS^-$, $p\text{-}CF_3C_6H_4S^-$ ($R_FS^-$), $PEt_3$, and $CN^-$ and has been utilized to define the competitive binding features of Mo and Fe atoms in a common cluster. The clusters **2** were originally synthesized in order to provide a labile binding site at the Mo atom. Inasmuch as FeMo-co appears to contain sulfur in no form but sulfide and lacks endogenous organic material,[17,19] the thiolate ligands in **2** have been replaced by chloride in the cluster $[MoFe_3S_4Cl_3(al_2cat)(solv)]^{2-}$ (**4**, solv = solvent). This modification preserves the net charge, a desirable feature inasmuch as FeMo-co is anionic,[19] and results in enhanced substitutional lability at the Fe sites, thereby providing a more meaningful assessment of competitive binding. Chloride is present in solutions of FeMo-co preparations and is a potential ligand for both Mo and Fe atoms. Also included in this report are the synthesis and structure of **4** as its THF adduct.

## Experimental Section

**Preparation of $(Et_4N)_2[MoFe_3S_4Cl_3(al_2cat)(THF)]\cdot0.5CH_3COCH_3$.** All operations were carried out under a pure dinitrogen atmosphere; solvents were degassed before use. Purification of solvents and reagents and a description of anaerobic procedures have been presented elsewhere.[3] A slurry of 2.15 g (1.05 mmol) of $(Et_4N)_4[Mo_2Fe_6S_8(SEt)_6(al_2cat)_2]$[6] in 400 mL of acetonitrile was cooled to 0 °C. A solution of 0.47 mL (6.33 mmol) of acetyl chloride in 100 mL of acetonitrile was added dropwise over an 80-min period to the well-stirred slurry. After the addition was completed, the cooling bath was removed and the homogeneous solution was stirred for 1 h at ambient temperature. After removal of volatile materials in vacuo, the residue was extracted with 100 mL of acetone. The filtered extract was reduced in vacuo to a volume of 30 mL. This solution was diluted with THF to a final volume of ~100 mL and maintained at −20 °C overnight. Crystallization was induced by scratching and was allowed to proceed overnight at 5 °C and then briefly at −20 °C. The product was collected by filtration, washed with THF, and dried in vacuo. Recrystallization from acetone/THF with cooling of the solution to 5 °C afforded 0.980 g (45%) of a purple microcrystalline solid. The $^1H$ NMR spectrum ($CD_3CN$, ~25 °C) contained a paramagnetically shifted resonance at −10.39 ppm due to the catecholate ring protons. Analytical and NMR data are consistent with an acetone hemisolvate. Anal. Calcd for $C_{32}H_{60}Cl_3Fe_3MoN_2O_3S_4\cdot0.5C_3H_6O$: C, 38.40; H, 6.06; Cl, 10.15; Fe, 15.99; Mo, 9.15; O, 5.34; N, 2.67; S, 12.24. Found: C, 38.88; H, 6.27; Cl, 10.19; Fe, 15.93; Mo, 9.00; O, 4.73 (by difference); N, 2.73; S, 12.27. Absorption spectrum (acetonitrile): $\lambda_{max}$ 491 ($\epsilon_M$ 5790), 296 (sh, 16 300), 241 nm (sh, 40 500). Recrystallization from 1:4 (v/v) *n*-butyronitrile/THF gave the acetone-free compound, as confirmed by $^1H$ NMR and limited analysis. Anal. Calcd for $C_{32}H_{60}Cl_3Fe_3MoN_2O_3S_4$: Fe, 16.44; Mo, 9.42; S, 12.59. Found: Fe, 16.34; Mo, 9.30; S, 12.35. Best results are obtained with use of freshly purified recrystallization solvents. After addition of the THF cosolvent, portions of the product frequently separated as an amorphous solid. This behavior can be minimized and a highly crystalline product obtained by avoidance of agitation of the solution during storage of the recrystallization solution at 5 °C.

**Table I.** Summary of Crystal Data, Intensity Collection, and Structure Refinement Parameters for $(Et_4N)_2[MoFe_3S_4Cl_3(C_{12}H_{12}O_2)(C_4H_8O)]$

| | |
|---|---|
| formula (mol wt) | $C_{32}H_{60}Cl_3Fe_3MoN_2O_3S_4$ (1018.90) |
| *a*, Å | 23.829 (5) |
| *b*, Å | 11.452 (3) |
| *c*, Å | 16.870 (3) |
| $\beta$, deg | 106.15 (2) |
| cryst system | monoclinic |
| *V*, Å$^3$ | 4419 (2) |
| *Z* | 4 |
| $d_{calcd}$, g/cm$^3$ | 1.53 |
| $d_{obsd}$, g/cm$^3$ [a] | 1.52 |
| space group | *C*2/*c* |
| cryst dimens,[b] mm | 0.30 × 0.20 × 0.06 |
| cryst faces | (100), ($\bar{1}00$), (010), ($0\bar{1}0$), (001), ($00\bar{1}$) |
| radiation | Mo $K\bar{\alpha}$ ($\lambda$ = 0.710 69 Å) |
| abs coeff $\mu$, cm$^{-1}$ | 16.25 |
| scan speed, deg/min | 2–29.3 ($\theta/2\theta$ scan) |
| scan range, deg | $2 + (2\theta_{K\alpha_1} - 2\theta_{K\alpha_2})$ |
| background/scan time ratio | 0.25 |
| data collected | 3°–40°, 40°–50° ($+h, +k, \pm l$) |
| unique data ($F_o^2 > 3\sigma(F_o^2)$) | 2451 |
| no. of variables | 247 |
| goodness of fit | 1.05 |
| *R*, % | 3.88 |
| $R_w$, % | 3.94 |

[a] Determined by flotation in $CCl_4$/cyclohexane. [b] Plate-shaped crystal.

**Ligand Substitution Reactions.** $(Et_4N)CN$[20] and $(Et_4N)(SPh)$[3] were prepared as described. $(Et_4N)(p\text{-}CF_3C_6H_4S)$ was obtained from $p\text{-}CF_3C_6H_4SH$[21] in a manner analogous to that for the benzenethiolate salt. Commercial $PEt_3$ (Strem) was used as received. All reactions were conducted under anaerobic conditions. Stock solutions containing ~10 mM cluster prepared from the $Et_4N^+$ salt of $[MoFe_3S_4Cl_3(al_2cat)(THF)]^{2-}$ and $CD_3CN$ or $Me_2SO\text{-}d_6$ were treated stepwise with known equivalents of the various ligands dissolved in the same solvent. $^1H$ (300 MHz) or $^{19}F$ (282.4 MHz) NMR spectra were recorded within 90 min of sample preparation on a Bruker WM-300 spectrometer at ambient probe temperature (~297 K). All measurements refer to equilibrium solutions. Chemical shifts at fields above and below those of the internal standards ($Me_4Si$, $PhCF_3$) are designated as positive and negative, respectively, consistent with a usual convention for paramagnetic molecules.

**Structure Determination of $(Et_4N)_2[MoFe_3S_4Cl_3(al_2cat)(THF)]$. Collection and Reduction of X-ray Data.** Long black needles of the title compound were grown by vapor diffusion of THF into a *n*-butyronitrile solution under slightly reduced pressure, followed by slow cooling. A crystal of suitable length was cleaved and mounted in a glass capillary with the aid of apiezon grease and the capillary flame-sealed under an argon atmosphere. Diffraction experiments were performed with a Nicolet R3M four-circle automated diffractometer with a Mo X-ray tube equipped with a graphite monochromator. Data collection parameters are summarized in Table I. The final orientation matrix and unit cell parameters were determined from 25 machine-centered reflections having $15 \leq 2\theta \leq 25°$. Selected $\omega$ scans displayed some structure, half-widths were consistently in the range of 0.28–0.32°, and the scans were well resolved from background. Three standard reflections, examined after every 60 measurements, showed no signs of decay during the course of the collection. Data reduction was carried out with the program XTAPE of the SHELXTL structure determination package (Nicolet XRD Corp., Fremont, CA); an analytical absorption correction was applied with the program X of SHELXTL structure determination package. The systematic absences *hkl* ($h + k \neq 2n$) and *h*0*l* ($l \neq 2n$) are consistent with monoclinic space groups *Cc* and *C*2/*c*. Simple *E* statistics favored the centric space group; the choice was confirmed by successful solution and refinement in space group *C*2/*c*.

---

(15) Wolff, T. E.; Berg, J. M.; Hodgson, K. O.; Frankel, R. B.; Holm, R. H. *J. Am. Chem. Soc.* **1979**, *101*, 4140.

(16) For other experiments and interpretations relevant to the Fe mean oxidation state in $[MoFe_3S_4]^{3+}$ clusters: cf. Christou, G.; Collison, D.; Garner, C. D.; Acott, S. R.; Mabbs, F. E.; Petrouleas, V. *J. Chem. Soc., Dalton Trans.* **1982**, 1575.

(17) For a review of FeMo-co properties: cf. Burgess, B. K.; Newton, W. E. In "Nitrogen Fixation: Chemical/Biochemical/Genetics Interface"; Muller, A., Newton, W. E., Eds.; Plenum Press: New York, 1983, in press.

(18) Nelson, M. J.; Levy, M. A.; Orme-Johnson, W. H. *Proc. Natl. Acad. Sci. U.S.A.* **1983**, *80*, 147.

(19) Yang, S.-S.; Pan, W.-H.; Friesen, G. D.; Burgess, B. K.; Corbin, J. L.; Stiefel, E. I.; Newton, W. E. *J. Biol. Chem.* **1982**, *257*, 8042.

(20) Webster, O. W.; Mahler, W.; Benson, R. E. *J. Am. Chem. Soc.* **1962**, *84*, 3678. Andreades, S.; Zahnow, E. W. *Ibid.* **1969**, *91*, 4181.

(21) Wong, G. B.; Kurtz, D. M., Jr.; Holm, R. H.; Mortenson, L. E.; Upchurch, R. G. *J. Am. Chem. Soc.* **1979**, *101*, 3078.

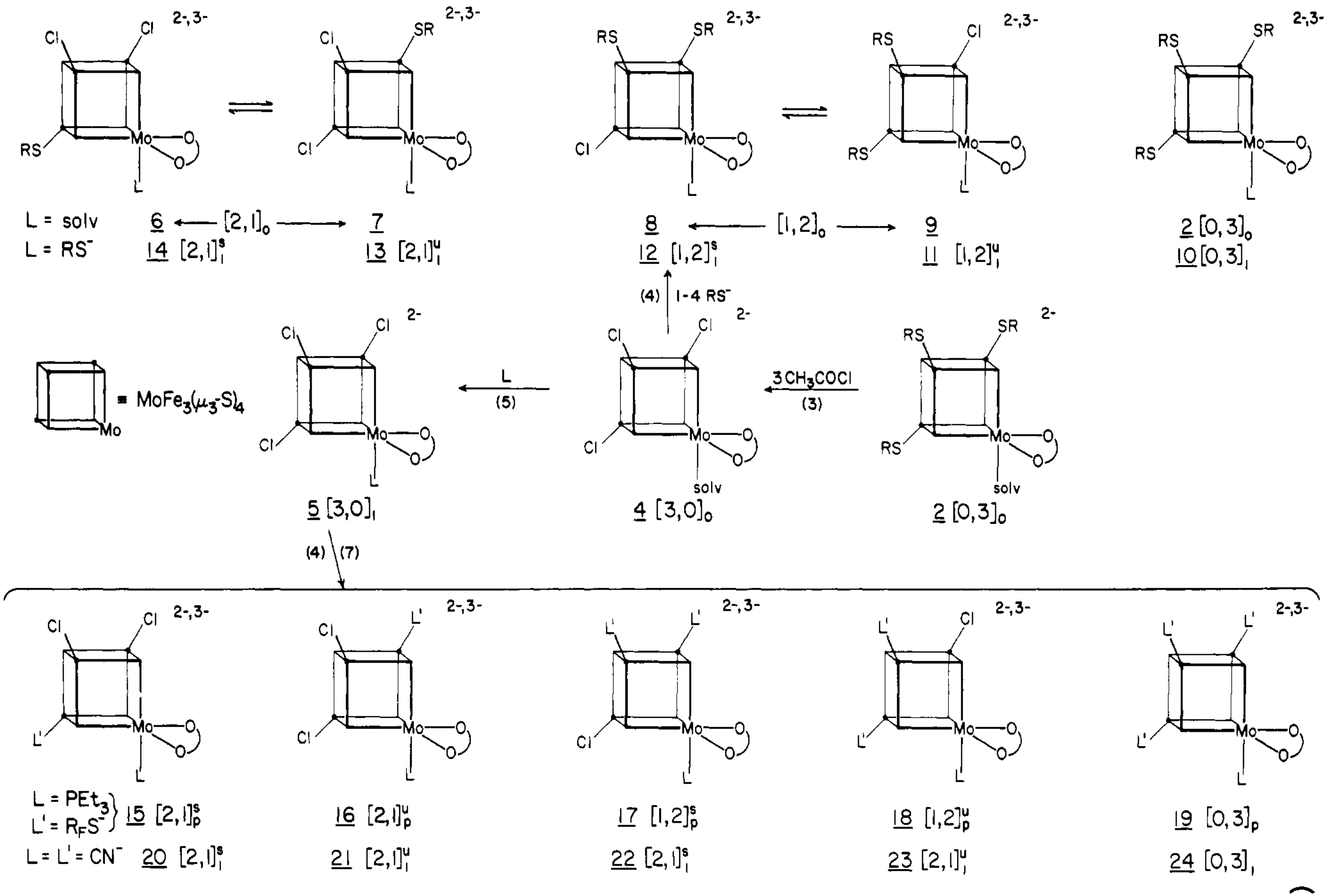

**Figure 1.** Schematic representations of reactions and structures of $MoFe_3S_4$ clusters with various sets of terminal ligands at Fe and Mo sites: O͡O = $al_2cat^{2-}$; L′ = solv (**2**, **6–9**), $RS^-$ (**10–14**), $PEt_3$ (**15–19**), $CN^-$ (**20–24**); L′ = $RS^-$ (**15–19**), $CN^-$ (**20–24**); R = Ph or $R_F$ ($p$-$C_6H_4CF_3$). Double arrows indicate species whose $m'$ and $m''$ sites are equilibrated by the fluxional process in Figure 4.

**Solution and Refinement of the Structure.** The direct methods option SOLV of the X program (vide supra) was employed. Trial positions for the Mo, Fe, and S atoms were taken from the *E* map derived from the phase set with the highest combined figure of merit. The remaining non-hydrogen atoms were determined by subsequent difference Fourier maps. The structure was refined by the blocked cascade least-squares method. Fixed contributions from the hydrogen atoms (C–H bond length of 0.96 Å) with thermal parameters set at 1.2 times that of the bonded carbon atom were included in the final stages of the refinement. All non-hydrogen atoms were refined with anisotropic thermal parameters except for the disordered terminal methylene carbon atom in the side chain of the $al_2cat^{2-}$ ligand. The asymmetric unit consists of half of the anion and 2 half-cations; the remaining atoms are generated by reflection symmetry. The disordered carbon atom (C(6)) was modeled with two sites whose total refined occupancies summed to unity. Additionally, the two sites were constrained to have a common isotropic temperature factor and to be equidistant from the methine carbon (C(5)). The final model converged to occupancies of 0.66 (1) and 0.34 (1) for sites A and B, respectively, with a bond length of 1.30 (1) Å to C(5). No H atom contribution was included for C(5). Unique data used in the refinement and final R factors are given in Table I. Positional parameters and selected interatomic distances and angles of the anion are presented in Tables II and III,[22] respectively.

## Results and Discussion

**Synthesis and Structure of $[MoFe_3S_4Cl_3(al_2cat)(THF)]^{2-}$.** We have previously shown that the clusters $[Fe_4S_4(SR)_4]^{2-}$ [23,24] and the double-cubanes $[Mo_2Fe_6(\mu\text{-}SR)_3(SR)_6]^{3-}$ [3,15] and $[Mo_2Fe_7S_8(\mu\text{-}SR)_6(SR)_6]^{3-}$ [3,25] react completely and irreversibly with *n* equiv of acetyl chloride, resulting in a roughly statistical distribution of clusters with $RS^-/Cl^-$ terminal ligand substitution and the formation of thioester. The analogous reaction 3 with

Table II. Positional Parameters for $[MoFe_3S_4Cl_3(al_2cat)(THF)]^{2-}$

| atom | *x* | *y* | *z* |
|---|---|---|---|
| Mo | 0.2841 (1)[a] | 0 | 0.2294 (1) |
| Fe(1) | 0.3579 (1) | 0.1193 (1) | 0.3597 (1) |
| Fe(2) | 0.4049 (1) | 0 | 0.2540 (1) |
| S(1) | 0.2830 (1) | 0 | 0.3678 (1) |
| S(2) | 0.4377 (1) | 0 | 0.3944 (1) |
| S(3) | 0.3457 (1) | 0.1609 (1) | 0.2250 (1) |
| Cl(1) | 0.3680 (1) | 0.2790 (2) | 0.4397 (1) |
| Cl(2) | 0.4777 (1) | 0 | 0.1956 (2) |
| O(1)[b] | 0.2150 (2) | 0.1126 (3) | 0.1942 (2) |
| C(1) | 0.1627 (2) | 0.0611 (5) | 0.1643 (3) |
| C(2) | 0.1109 (3) | 0.1245 (5) | 0.1317 (4) |
| C(3) | 0.0582 (3) | 0.0588 (6) | 0.1018 (4) |
| C(4) | 0.1109 (3) | 0.2562 (6) | 0.1247 (4) |
| C(5) | 0.1007 (4) | 0.3040 (8) | 0.0389 (7) |
| C(6a)[c] | 0.0965 (7) | 0.2448 (15) | −0.0283 (9) |
| C(6b) | 0.0577 (10) | 0.3773 (22) | 0.0166 (19) |
| O(2) | 0.2691 (3) | 0 | 0.0856 (3) |
| C(7) | 0.2566 (3) | 0.1032 (6) | 0.0356 (4) |
| C(8) | 0.2324 (5) | 0.0616 (7) | −0.0501 (5) |

[a] Estimated standard deviations in parentheses in this and succeeding tables. [b] The labeling schemes for the $al_2cat^{2-}$ and THF ligands are the following

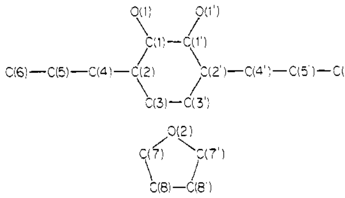

[c] Disordered atom.

---

[22] See paragraph at the end of this article regarding available supplementary material.

[23] Wong, G. B.; Bobrik, M. A.; Holm, R. H. *Inorg. Chem.* **1978**, *17*, 578.

[24] Johnson, R. W.; Holm, R. H. *J. Am. Chem. Soc.* **1978**, *100*, 5338.

[25] Wolff, T. E.; Berg, J. M.; Power, P. P.; Hodgson, K. O.; Holm, R. H. *Inorg. Chem.* **1980**, *19*, 430.

$$[MoFe_3S_4(SEt)_3(al_2cat)(MeCN)]^{2-} + 3CH_3COCl \rightarrow [MoFe_3S_4Cl_3(al_2cat)(MeCN)]^{2-} + 3CH_3COSEt \quad (3)$$

3 equiv of electrophile in acetonitrile affords the solvated cluster **4** which, after recrystallization from acetone/THF or *n*-PrCN/THF, was isolated as the THF adduct. This and most other reactions considered subsequently are shown in Figure 1 together with schematic depictions of reactant and product clusters. The designation **4** refers, as appropriate, to a THF, $Me_2SO$, or MeCN solvate cluster.

The structure of $[MoFe_3S_4Cl_3(al_2cat)(THF)]^{2-}$ (**4**) is presented in Figure 2. Selected interatomic distances and angles are collected in Table III. Structures of a number of $MoFe_3S_4$ clusters have been described previously.[1,2,4–6,8,15,25] Of these the structure of the single-cubane $[MoFe_3S_4(S\text{-}p\text{-}C_6H_4Cl)_4(al_2cat)]^{3-}$ (**3**, R = *p*-$C_6H_4Cl$, L = *p*-$ClC_6H_4S^-$)[4,8] is the most closely related to that of the chloro-substituted cluster. The leading structural features of **4** are briefly summarized together with certain comparisons with **3**. (i) A crystallographically imposed mirror plane bisects the catecholate chelate ring and contains the atoms Mo, S(1,2), Fe(2), Cl(2), and O(2). (ii) The $C_s$ cluster symmetry requires two types of Fe sites, *m'*(Fe(2)), in the mirror plane, and *m''*(Fe(1,1')), off and related by the plane. The structure of **3** has no imposed symmetry, but its $[MoFe_3S_4]^{3+}$ core approaches $C_s$. (iii) The six core faces are nonplanar rhombs, a feature that extends to all $MoFe_3S_4$ cubanes. (iv) Each Fe atom occupies an approximately tetrahedral site; the Fe–Cl distance at the *m'* site is 0.026 Å shorter than those at the *m''* sites. (v) The Mo atom exhibits a distorted octahedral geometry; a catecholate chelate ring, roughly coplanar with the MoS(3,3')Fe(2) core face, and a THF molecule complete the coordination external to the core. (vi) Corresponding bond distances in **3** and **4** differ by $\lesssim$0.06 Å. Of these differences the most interesting are the reversals in Mo–S(1), Mo–O(1), and Fe(2)–S(2) values, which are 0.062, 0.035, and 0.040 Å shorter, respectively, in **4**. The first two of these appear to arise directly from the coordination of a hard neutral ligand (THF) in **4** compared to an anionic polarizable ligand ($RS^-$) in **3**. (vii) The C(1)–O(1) distance of 1.343 (6) Å and ring C–C distances are compatible with the presence of a catecholate dianion ligand rather than an oxidized form.[26] Both **3** and **4** contain isoelectronic cores whose volumes of 9.56 and 9.37 $Å^3$, respectively, differ by 1.5%, a variation which reflects the dimensional differences noted in (vi). (viii) In terms of binding strength the Mo–O(2) distance of 2.352 (6) Å is difficult to assess owing to the lack of appropriate Mo(III,IV)–O distances to neutral donors for comparison. It is substantially longer than the mean Mo–N distance (2.19 (3) Å) in *mer*-$MoCl_3(py)_3$[27] and close to the Mo–O (neutral ligand) values in $[MoO(salen)(MeOH)]^{1+}$[28] (2.33–2.36 Å) and $[MoOCl_4(THF)]^{1-}$[29] (2.331 (5) Å), among others, where the neutral ligand is subject to the trans influence of an oxo atom. In $Mo_2O_3(NH)(S_2P(OEt)_2)_2{\cdot}THF$ the Mo–O(THF) distance is 2.633 (3) Å and THF is reported to be readily lost from the crystals at room temperature.[30] This behavior is not found with the $Et_4N^+$ salt of **4**. Elsewhere we have observed, from more relevant metric comparisons, that the Mo–SR bond in **3** (2.600 (3) Å) is unexpectedly long.[8] Lastly, the proof of coordinated THF in **4** supports the existence of solvated clusters **2** in solution, no others of which have yet proven attainable as solids because of preferential crystallization of the double-cubanes **1** upon attempted isolation.

**Solution Properties of Clusters 2–4.** That property of prime importance to the present study is the sensitivity of the isotropically shifted $^1H$ and $^{19}F$ NMR resonances of ligands at the Mo and Fe sites to the composition of the total ligand set and the symmetry of the cluster. Some examples of this behavior, which is more fully exploited here, have been presented.[4,6–8] The $^1H$ spectrum of **4** in acetonitrile, provided in Figure 3, consists of a sharp $al_2cat$ ring proton resonance at −10.39 ppm and allyl signals near those

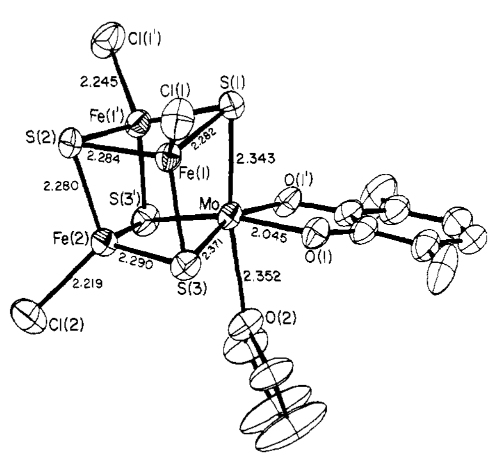
$[MoFe_3S_4Cl_3((C_3H_5)_2cat)(THF)]^{2-}$

**Figure 2.** Structure of $[MoFe_3S_4Cl_3(al_2cat)(THF)]^{2-}$ as its $Et_4N^+$ salt, showing the atom labeling scheme, 50% probability ellipsoids, and selected bond distances (vinyl groups of the catecholate ligand are omitted). Primed and unprimed atoms are related by an imposed mirror plane.

**Table III.** Selected Interatomic Distances (Å) and Angles (deg) in $[MoFe_3S_4Cl_3((C_3H_5)_2cat)(THF)]^{2-}$

| | | | |
|---|---|---|---|
| Distances | | | |
| Mo–S(1) | 2.343 (2) | Fe(1)···S(3') | 3.897 (2) |
| Mo–S(3) | 2.371 (2) | Fe(2)···S(1) | 3.904 (3) |
| mean | 2.36 (2)[a] | mean | 3.90 (0) |
| Mo···S(2) | 3.936 (2) | O(1)···O(1') | 2.578 (7) |
| Mo–O(1) | 2.045 (4) | O(1)–C(1) | 1.343 (6) |
| Mo–O(2) | 2.352 (6) | C(1)–C(1') | 1.401 (11) |
| | | C(1)–C(2) | 1.406 (8) |
| Fe(1)–S(1) | 2.282 (2) | C(2)–C(3) | 1.430 (8) |
| Fe(1)–S(2) | 2.283 (2) | C(3)–C(3') | 1.347 (13) |
| Fe(2)–S(3) | 2.290 (2) | C(2)–C(4) | 1.513 (9) |
| Fe(1)–S(3) | 2.261 (2) | C(4)–C(5) | 1.502 (13) |
| Fe(2)–S(2) | 2.280 (2) | C(5)–C(6)[b] | 1.30 (1) |
| mean | 2.28 (1) | | |
| | | S(1)···S(2) | 3.590 (3) |
| Fe(1)–Cl(1) | 2.245 (2) | S(1)···S(3) | 3.667 (3) |
| Fe(2)–Cl(2) | 2.219 (3) | S(2)···S(3) | 3.591 (2) |
| mean | 2.24 (2) | S(3)···S(3') | 3.686 (3) |
| Mo···Fe(1) | 2.765 (1) | mean | 3.62 (7) |
| Mo···Fe(2) | 2.794 (1) | C(7)–O(2) | 1.434 (7) |
| mean | 2.78 (2) | C(7)–C(8) | 1.478 (10) |
| Fe(1)···Fe(2) | 2.725 (1) | C(8)–C(8') | 1.411 (16) |
| Fe(1)···Fe(1') | 2.733 (2) | | |
| mean | 2.728 (5) | | |
| Bond Angles | | | |
| O(1)–Mo–O(1') | 78.2 (2) | Fe(1)–Mo–Fe(2) | 58.7 (0) |
| O(1)–Mo–S(3) | 87.5 (1) | Fe(1)–Mo–Fe(1') | 59.2 (0) |
| S(3)–Mo–S(3') | 102.0 (1) | | |
| S(1)–Mo–O(1) | 93.3 (1) | S(1)–Fe(1)–S(2) | 103.7 (1) |
| S(1)–Mo–S(3) | 102.1 (1) | S(2)–Fe(1)–S(3) | 104.4 (1) |
| O(1)–Mo–O(2) | 79.7 (2) | S(1)–Fe(1)–S(3) | 107.6 (1) |
| O(2)–Mo–S(3) | 83.4 (1) | S(2)–Fe(2)–S(3) | 103.6 (1) |
| | | S(3)–Fe(2)–S(3') | 107.2 (1) |
| O(1)–Mo–S(3') | 159.5 (1) | Cl(1)–Fe(1)–S(1) | 114.0 (1) |
| O(2)–Mo–S(1) | 171.0 (2) | Cl(1)–Fe(1)–S(2) | 113.0 (1) |
| Mo–S(1)–Fe(1) | 73.3 (1) | Cl(1)–Fe(1)–S(3) | 113.3 (1) |
| Mo–S(3)–Fe(2) | 73.6 (1) | Cl(2)–Fe(2)–S(3) | 114.6 (1) |
| Mo–S(3)–Fe(1) | 73.5 (1) | Cl(2)–Fe(2)–S(2) | 112.2 (1) |
| Fe(1)–S(1)–Fe(1') | 73.6 (1) | | |
| Fe(1)–S(2)–Fe(1') | 73.5 (1) | | |
| Fe(1)–S(2)–Fe(2) | 73.3 (1) | | |
| Fe(1)–S(3)–Fe(2) | 73.5 (1) | | |

[a] The standard deviation of the mean was estimated as $\sigma \approx s = [(\Sigma x_i^2 - n\bar{x}^2)/(n-1)]^{1/2}$; weighted values under $C_s$ symmetry are given. [b] C(6) is disordered.

---

[26] Pierpont, C. G.; Buchanan, R. M. *Inorg. Chem.* **1982**, *21*, 652; *Coord. Chem. Rev.* **1981**, *38*, 45.

[27] Brenčič, J. V. *Z. Anorg. Allg. Chem.* **1974**, *403*, 218.

[28] Gheller, S. F.; Bradbury, J. R.; Mackay, M. F.; Wedd, A. G. *Inorg. Chem.* **1981**, *20*, 3899.

[29] Bird, P. H.; Wickramasinghe, W. A. *Can. J. Chem.* **1981**, *59*, 2879.

[30] Edelblut, A. W.; Haymore, B. L.; Wentworth, R. A. D. *J. Am. Chem. Soc.* **1978**, *100*, 2250.

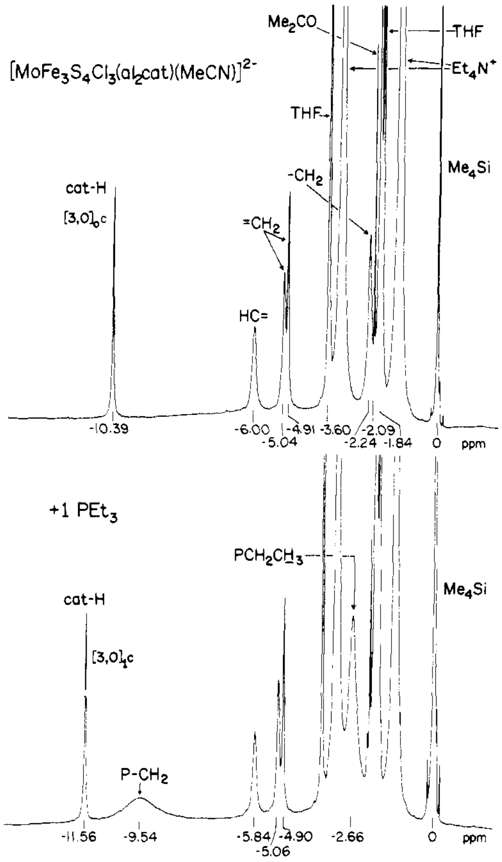

**Figure 3.** $^1$H NMR spectra of 11 mM $[MoFe_3S_4Cl_3(al_2cat)(MeCN)]^{2-}$ and its reaction product with 1 equiv of $PEt_3$ in $CD_3CN$ solution (signal assignments are indicated).

of the free ligand. Also evident are the resonances of the acetone of crystallization and of free THF, showing that the cluster exists as the acetonitrile solvate **4**. Similar behavior is observed in $Me_2SO$ where the catecholate signal of the solvated cluster occurs at −11.86 ppm, illustrating the sensitivity of ring proton shifts to the nature of the Mo terminal ligand. $[MoFe_3S_4Cl_3(al_2cat)(MeCN)]^{2-}$ is further characterized by a visible absorption band at 491 nm ($\epsilon_M$ 5790), a solution magnetic moment of 4.10 $\mu_B$ (~297 K), and a reversible one-electron reduction at −1.02 V vs. SCE (cyclic voltammetry, 0.1 M $n$-$Bu_4NCl$, 100 mV/s). An irreversible reduction at $E_{p,c} = -1.84$ V was also observed.

NMR spectra of solvated **2** and ligated **3** clusters exhibit a striking difference whose recognition is important in the spectral interpretations which follow. Spectra of the former exhibit one set of R group resonances whereas those of the latter exhibit two sets in a 2:1 intensity ratio consistent with cluster $C_s$ symmetry. A brief explanation has been given earlier[4,6,8] and is provided more explicitly here with the aid of Figure 4. The proposed process consists of solvent dissociation, chelate ring reorientation to a degenerate position roughly coplanar with a second core face, and solvent rebinding. Repetitions of this process will equilibrate in-mirror ($m'$) and off-mirror ($m''$) sites and afford a cluster of time-averaged trigonal symmetry. This fluxional behavior, which persists in acetonitrile solutions at ~240 K,[6] renders the isomers **6**/**7** and **8**/**9** (Figure 1) indistinguishable, whereas isomers with nonlabile ligands at the Mo site are detectable.

**Ligand Substitution Reactions.** Those reactions involving a single type of added ligand L can be represented by the generalized reaction 4, in which solv = MeCN or $Me_2SO$, $a \leq 3$ is the number

$$[MoFe_3S_4Cl_3(al_2cat)(solv)]^{2-} + (a + b)L^{0,1-} \rightarrow [MoFe_3S_4Cl_{3-a}L_a(al_2cat)L_b]^{2-,3-} + aCl^- + b\,solv \quad (4)$$

of L at Fe sites, and $b = 0,1$ is the number of L at the Mo site. Clusters are designated numerically or as $[3 - a,a]_b$. NMR signal assignments are given as $[3 - a,a]_bq$ where q = c (catecholate ring protons), $m$ (for $b = 0$; meta signals of ligands at Fe sites in effective trigonal symmetry), and $m'$ or $m''$ (for $b = 1$; meta signals from distinct Fe sites in nonfluxional clusters). When ligands are at a Mo site, q = Mo. Cluster designations are given in Figure 1, to which reference can be made in the following considerations of individual reaction systems.

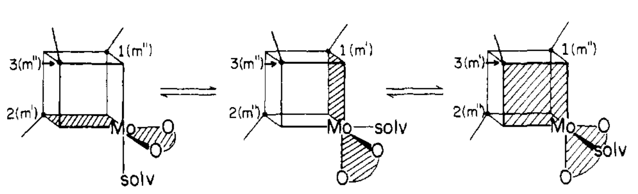

**Figure 4.** Proposed rearrangement process of solvated clusters resulting in equilibration of $m'$ and $m''$ sites on the NMR time scale. Shaded chelate rings and $MoFeS_2$ core faces are approximately coplanar; labels 1, 2, and 3 are absolute designations of Fe sites.

**(a) 4 + $PEt_3$.** Treatment of the cluster in acetonitrile with 1.0 equiv of the phosphine results in a shift of the visible band of **4** to 474 nm ($\epsilon_M$ 4870). The NMR spectrum of the reaction product is shown in Figure 3. The appearance of $[3,0]_1c$ at −11.56 ppm and of broadened, isotropically shifted phosphine signals, together with the absence of the features of **4**, demonstrate quantitative formation of the phosphine adduct **5** (L = $PEt_3$) in reaction 5,

$$[MoFe_3S_4Cl_3(al_2cat)(MeCN)]^{2-} + PEt_3 \rightarrow [MoFe_3S_4Cl_3(al_2cat)(PEt_3)]^{2-} + MeCN \quad (5)$$

an example of reaction 4 with $a = 0$ and $b = 1$. Use of 0.5 equiv of $PEt_3$ gave equimolar amounts of **4** and **5**; addition of up to 3 equiv of the phosphine resulted in line broadening of $[3,0]_1c$, indicating the onset of an exchange process. No signals attributable to additional clusters were observed. The same behavior was found with 0.5–3.0 equiv of $PEt_3$ in $Me_2SO$ solution ($[3,0]_1c$ at −11.32 ppm). In contrast the clusters **3** with L = $RS^-$ and $RO^-$ are fully dissociated in this solvent.[6]

In the reaction systems which follow, signal assignments are based on the growth and decay of relative integrated intensities as the equivalent of added ligand was varied. When L = $PhS^-$, isotropic interactions shift the $m$-H signals to low field, in the vicinity of catecholate ring proton signals, and $o$-H and $p$-H resonances to high field. Only the better resolved, low-field regions are shown. In a number of systems small amounts of $[Fe_2S_2(SR)_4]^{2-}$ [7,31] (d$^{2-}$), $[Fe_4S_4(SR)_4]^{2-}$ [7,21,32] (t$^{2-}$), and $[Fe(SR)_4]^{2-}$ [7,33,34] ($m$-H −22.3 ppm; not shown) with R = Ph or $p$-$C_6H_4CF_3$ were produced by degradation of the $MoFe_3S_4$ clusters and were identified by comparison with authentic samples. Another conceivable degradation product, $[(RS)_2FeS_2MoS_2]^{2-}$,[7,35] was not detected in any system.

**(b) 4 + $PhS^-$.** Spectra of the reaction products of **4** and 1–4 equiv of $PhS^-$ in $Me_2SO$ are shown in Figure 5. With 1.0 equiv of thiolate seven catecholate + $m$-H resonances (signals 1–7) are observed, consistent with a mixture of all possible substitution products, **6**/**7**, **8**/**9**, and **2**. These species have different extents of substitution at Fe sites, and all are solvated at the Mo site. Substitution is complete at 3.0 equiv; that no further spectral change occurs upon addition of another equiv of $PhS^-$ is shown by the presence of free thiolate signals 8 and 9. Progressive thiolate substitution effects a monotonic shift of the $[3 - a,a]_0c$ resonances to high field. The final spectrum corresponds to $[MoFe_3S_4(SPh)_3(al_2cat)(Me_2SO)]^{2-}$ (**2**) whose complete spectrum, obtained from an authentic sample of **1** (R = Ph), is given elsewhere.[6]

---

(31) Reynolds, J. G.; Holm, R. H. *Inorg. Chem.* **1980**, *19*, 3257.

(32) Reynolds, J. G.; Laskowski, E. J.; Holm, R. H. *J. Am. Chem. Soc.* **1978**, *100*, 5315.

(33) Hagen, K. S.; Reynolds, J. G.; Holm, R. H. *J. Am. Chem. Soc.* **1981**, *103*, 4054.

(34) Coucouvanis, D.; Swenson, D.; Baenziger, N. C.; Murphy, C.; Holah, D. G.; Sfarnas, N.; Simopoulos, A.; Kostikas, A. *J. Am. Chem. Soc.* **1981**, *103*, 3350.

(35) Coucouvanis, D.; Stremple, P.; Simhon, E. D.; Swenson, D.; Baenziger, N. C.; Draganjac, M.; Chan, L. T.; Simopoulos, A.; Papaefthymiou, V.; Kostikas, A.; Petrouleas, V. *Inorg. Chem.* **1983**, *22*, 293. Tieckelmann, R. H.; Silvis, H. C.; Kent, T. A.; Huynh, B. H.; Waszczak, J. V.; Teo, B.-K.; Averill, B. A. *J. Am. Chem. Soc.* **1980**, *102*, 5550.

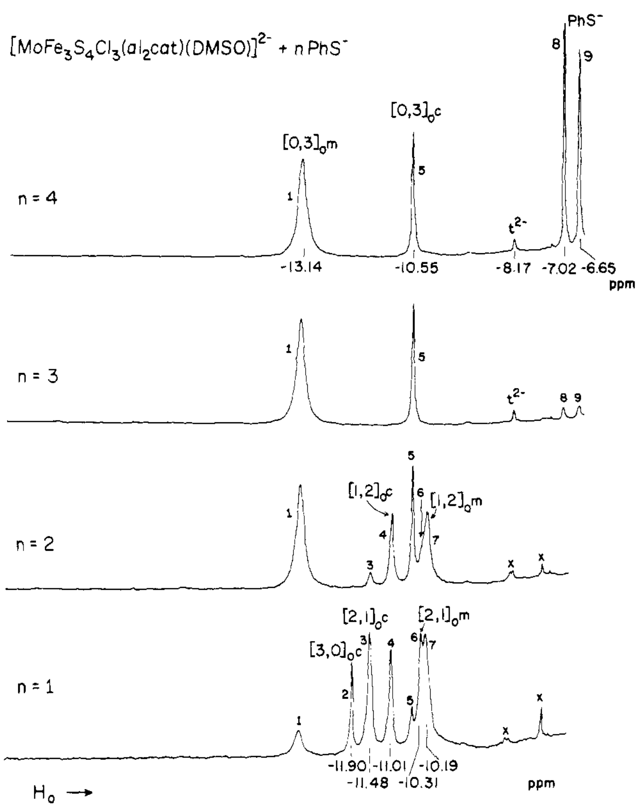

**Figure 5.** $^1H$ NMR spectra ($Me_2SO$-$d_6$ solutions) of the reaction products of 15 mM $[MoFe_3S_4Cl_3(al_2cat)(Me_2SO)]^{2-}$ with 1–4 equiv of $(Et_4N)(SPh)$. Signal assignments are indicated ($t^{2-} = [Fe_4S_4(SPh)_4]^{2-}$, x = unidentified resonance). For this and subsequent reaction systems the downfield spectral regions are shown and spectra are not plotted with constant amplitudes.

Spectra of reaction systems in acetonitrile with 1–4 equiv of $PhS^-$ are presented in Figure 6. With 1.0 equiv signals 1–7 correspond to the same species formed in $Me_2SO$ solution; chemical shifts do not follow the same order. With 2.0 equiv of thiolate the proportion of monosubstituted clusters **6**/**7** decreases and no new species are observed. At this point the situation is the same as in $Me_2SO$, all substitution having occurred at Fe sites. This result was further supported by the ligand scrambling reaction (6). When the clusters were combined in 2:1 and 1:2 ratios the

$$[MoFe_3S_4Cl_3(al_2cat)(MeCN)]^{2-} + [MoFe_3S_4(SPh)_3(al_2cat)(MeCN)]^{2-} \rightarrow 2[MoFe_3S_4Cl_{3-a}(SPh)_a(al_2cat)(MeCN)]^{2-} \quad (6)$$

NMR spectra of the reaction systems were identical with those of the 1.0 and 2.0 equiv reaction products, respectively. At 3.0 equiv of thiolate the predominant species is the solvated cluster **2**, and five new signals (8–12) have emerged. In the 4.0 equiv system there is a discontinuous change. All features of **2** are absent, and all resonances are assignable to the fully ligated cluster **10**. This species is not fluxional, resulting in resolution (by 6.9 ppm) of *m'* and *m''* resonances. The mean weighted value of these resonances (−13.0 ppm) is very close to the −13.4 ppm shift of fluxional **2**. Signals 11 (*o*-H) and 12 (*m*- + *p*-H) arise from the Mo–SPh ligand of **10**. The spectrum assigned to **10** is essentially identical with that of the structurally authenticated cluster with R = $p$-$C_6H_4Cl$ and L = $p$-$ClC_6H_4S^-$.[4,8] Inasmuch as only one set of *m'*/*m''* resonances was observed, the Mo-ligated, incompletely substituted clusters **11**–**14** were not formed in detectable amounts. In this system thiolate binding at Fe sites is virtually complete prior to binding at the Mo site.[36]

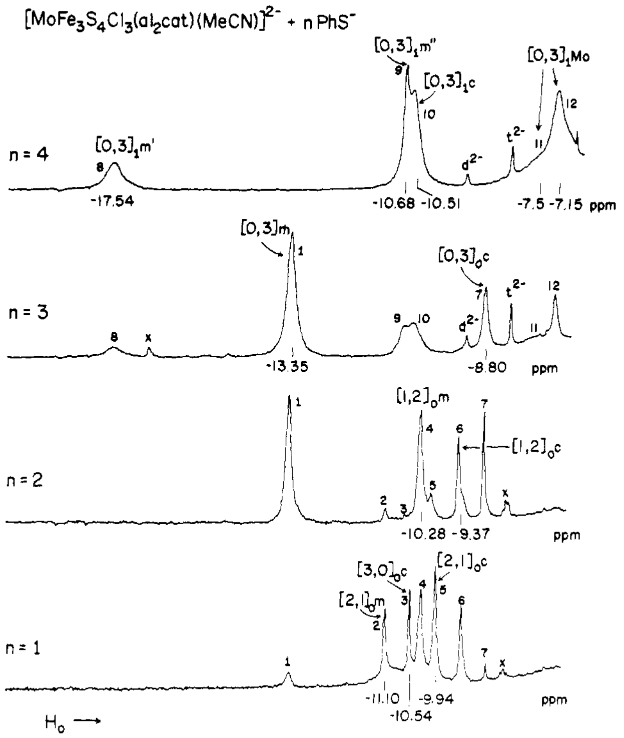

**Figure 6.** $^1H$ NMR spectra ($CD_3CN$ solutions) of the reaction products of 13 mM $[MoFe_3S_4Cl_3(al_2cat)(MeCN)]^{2-}$ with 1–4 equiv of $(Et_4N)(SPh)$. Signal assignments are indicated ($t^{2-} = [Fe_4S_4(SPh)_4]^{2-}$, $d^{2-} = [Fe_2S_2(SPh)_4]^{2-}$, x = unidentified resonance).

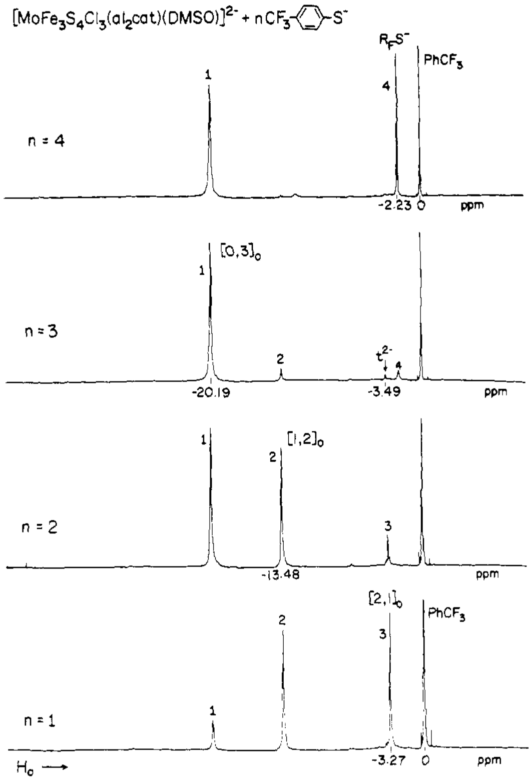

**Figure 7.** $^{19}F$ NMR spectra ($Me_2SO$-$d_6$ solutions) of the reaction products of 12 mM $[MoFe_3S_4Cl_3(al_2cat)(Me_2SO)]^{2-}$ with 1–4 equiv of $(Et_4N)(SR_F)$. Signal assignments are indicated ($t^{2-} = [Fe_4S_4(SR_F)_4]^{2-}$).

$^1H$ NMR spectra of the preceding two systems are sufficient to demonstrate mixed-ligand and fully substituted clusters as products of reaction 4 with L = $PhS^-$. Owing to the fluxional nature of the solvated clusters and lack of adequate signal resolution in some cases, these reaction systems are not entirely suitable for detection and quantitation of all possible reaction products.

---

[36] The presence of some **10** together with the majority species **2** in the 3 equiv system may be a consequence of a small excess of $PhS^-$ and/or a decomposition process that liberates $PhS^-$. That some cluster degradation has occurred is indicated by the presence of minor amounts of $d^{2-}$ and $t^{2-}$.

Table IV. Distribution of Product Clusters in Reactions of $[MoFe_3S_4Cl_3(al_2cat)(solv)]^{2-}$ (**4**) and $[MoFe_3S_4Cl_3(al_2cat)(PEt_3)]^{2-}$ (**5**) with *n* Equiv of $R_FS^-$

| | | *n* equiv | | |
|---|---|---|---|---|
| system | cluster | $1^a$ | $2^a$ | 3 |
| **4**/$Me_2SO$ (MeCN) | $[2,1]_0$ (**6**/**7**) | 0.59 (0.63)$^b$ | 0.18 | *c* |
| | $[1,2]_0$ (**8**/**9**) | 0.34 (0.32) | 0.41 | 0.09 |
| | $[0,3]_0$ (**2**) | 0.07 (0.05) | 0.41 | 0.91 |
| **5** (L = $PEt_3$)/MeCN | $[2,1]_p{}^s$ (**15**) | 0.06 | 0.03 | *c* |
| | $[2,1]_p{}^u$ (**16**) | 0.57 | 0.16 | *c* |
| | $[1,2]_p{}^s$ (**17**) | 0.21 | 0.30 | 0.06 |
| | $[1,2]_p{}^u$ (**18**) | 0.11 | 0.16 | *c* |
| | $[0,3]_p$ (**19**) | 0.05 | 0.35 | 0.94 |

[a] Statistical product ratios for *n* = 1 (2) equiv of thiolate assuming three identical Fe sites: [2,1]/[1,2] = 2 (0.5), [2,1]/[0,3] = 12 (0.747), [1,2]/[0,3] = 6 (1.5). [b] MeCN solution. [c] Not detectable.

Systems containing **4** and the nonlabile phosphine adduct **5** (L = $PEt_3$) with $R_FS^-$ are more effective in this respect.

**(c) 4 + $R_FS^-$.** $^{19}F$ spectra of this system in $Me_2SO$ with 1–4 equiv of thiolate, provided in Figure 7, are fully resolved and readily interpreted. The appearance of signals 1–3 in the 1 and 2 equiv spectra reveal formation of **6**/**7**, **8**/**9**, and **2**. At 3 equiv of thiolate fully substituted **2** is the dominant product, and at 4 equiv it is the exclusive product. Species mole fractions formed with 1–3 equiv of $R_FS^-$, obtained from normalized signal intensities, are given in Table IV.

**(d) 5 (L = $PEt_3$) + $R_FS^-$.** Clusters in this system are formed by reaction 7, a case of reaction 4 with *b* = 1 and $L_a \neq L_b$.

$$[MoFe_3S_4Cl_3(al_2cat)(PEt_3)]^{2-} + aR_FS^- \rightarrow [MoFe_3S_4Cl_{3-a}(R_FS)_a(al_2cat)(PEt_3)]^{2-} + aCl^- \quad (7)$$

Because of the presence of two types of ligands, signal assignments of possible product clusters **15**–**19** (Figure 1) are designated as $[3 - a,a]_p{}^rq$, where p = Mo-bound phosphine and r = s (symmetrical, $C_s$) or u (unsymmetrical). The u isomers **16** and **18**, which are chiral, have a statistical weight of 2 vs. their s counterparts **15** and **17**, a relevant factor inasmuch as all clusters in this system are nonfluxional. $^{19}F$ NMR spectra, whose resonances cover the range of ca. +4 to −34 ppm, are shown in Figure 8 for this reaction system in acetonitrile. The 1 and 2 equiv spectra exhibit signals 1–7, consistent with the seven L′ environments in clusters **15**–**19**. Signals 1 and 4 of fully substituted **19** are assigned from the 3 and 4 equiv spectra; the *m′* and *m″* environments are resolved by 22.8 ppm. In the 1 equiv spectrum signal 7 is assigned to the monosubstituted u isomer **16** on the basis of statistical weights. The less intense signal 3 is attributed to the s isomer **15**. This pair is diminished upon addition of a second equiv of thiolate and relative to it signals 2, 5, and 6 become more prominent and thus arise from disubstituted species. The equal intensities of signals 2 and 6 require assignment to the u isomer **18**. From the spectrum of **19** the former signal is ascribed to the ligand at the *m′* site. Signal 5 originates from the s isomer **17**. Mean weighted chemical shfits calculated from these assignments are −3.85 (**15**/**16**), −12.64 (**17**/**18**), and −18.98 (**19**) ppm. The favorable comparison of these values with those in Figure 7 for fluxional $[3 - a,a]_0$ clusters with the same *a* index further supports the assignments. Product cluster distributions are summarized in Table IV.

With the formation and signal assignments of fluxional and nonfluxional clusters established, attention is directed to the $^{19}F$ spectra of the system **4**/$R_FS^-$ in acetonitrile presented in Figure 9. As demonstrated by the results for the system **4**/PhS$^-$ in Figure 6 and by reaction 2, which has been employed on a preparative basis,[4,8] this solvent is less competitive for the Mo binding site than is $Me_2SO$. Signals 1, 5, and 8 are readily assigned to fully substituted **10** from the 3 and 4 equiv spectra and from a previous spectrum of the authentic cluster generated from **2** (R = $R_F$) by reaction 2.[7] The *m′* and *m″* shifts of **10** are close to those of **19**. The pattern of intensity changes of signals 7, 4, and 3 as equivalent of thiolate is increased and the similarities of their chemical shifts with the unambiguously assigned signals in the **4**/$R_FS^-$ system in $Me_2SO$ (Figure 7) leads to their assignment to the fluxional clusters **6**/**7**, **8**/**9**, and **2**, respectively, in order of increasing thiolate substitution. Further chemical shift similarities, of signals 2 and 6 to those of the phosphine-ligated clusters **17** and **18** (Figure 8), supports assignments to the disubstituted nonfluxional clusters **11** and **12**, respectively. The *m″* resonance of the u isomer **11**,

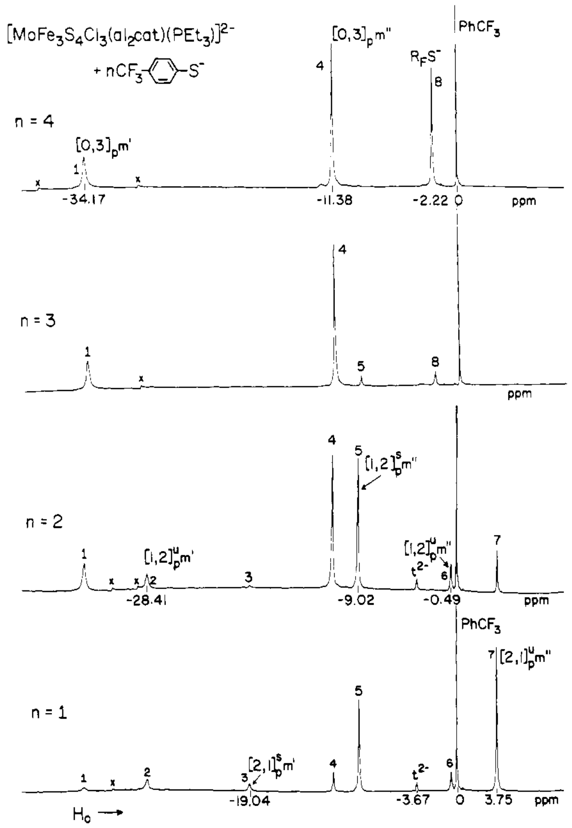

**Figure 8.** $^{19}F$ NMR spectra ($CD_3CN$ solutions) of the reaction products of 14 mM $[MoFe_3S_4Cl_3(al_2cat)(PEt_3)]^{2-}$ with 1–4 equiv of $(Et_4N)(SR_F)$. Signal assignments are indicated ($t^{2-} = [Fe_4S_4(SR_F)_4]^{2-}$, x = quadrature image).

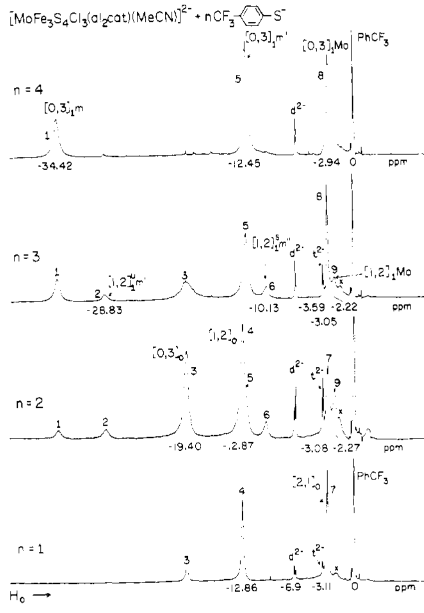

**Figure 9.** $^{19}F$ NMR spectra ($CD_3CN$ solutions) of the reaction products of 14 mM $[MoFe_3S_4Cl_3(al_2cat)(MeCN)]^{2-}$ with 1–4 equiv of $(Et_4N)(SR_F)$. Signal assignments are indicated ($t^{2-} = [Fe_4S_4(SR_F)_4]^{2-}$, $d^{2-} = [Fe_2S_2(SR_F)_{4-n}Cl_n]^{2-}$, x = unidentified resonance).

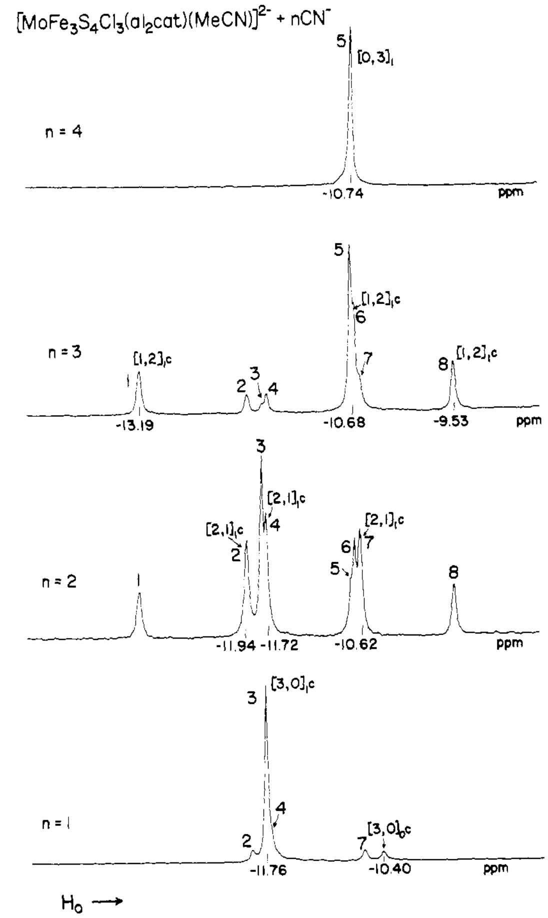

**Figure 10.** $^1H$ NMR spectra ($CD_3CN$ solutions) of the reaction products of 11 mM $[MoFe_3S_4Cl_3(al_2cat)(MeCN)]^{2-}$ with 1-4 equiv of $(Et_4N)CN$. Signal assignments are indicated.

expected near −1 ppm, either is the signal "*x*" or its obscured by other absorptions. On the basis of the chemical shift of the $Mo{-}SR_F$ ligand in **10** (−2.94 ppm), signal 9 is assigned to the corresponding ligand in **11** and **12**. There is no evidence for the formation of monosubstituted Mo-ligated **13** and **14**; in particular, the *m″* signal of the u isomer **13** expected at or above ~0 ppm is clearly absent. In this system substitution at Fe sites need not be complete prior to detectable binding at the Mo site. However, the clusters **11** and **12** are clearly minor constituents in the 2 and 3 equiv systems and are absent in the 1 and 4 equiv cases. Because of overlap of certain signals product cluster distributions cannot be accurately quantitated for 2 and 3 equiv systems.

**(e) 4 + $CN^-$.** Reaction of **4** with 1.0 equiv of $CN^-$ in acetonitrile results in the appearance of absorption bands at 298 (sh) and 472 ($\epsilon_M$ 5520) nm, a single $\nu_{CN}$ (2112 $cm^{-1}$),[37] and the intense sharp catecholate resonance 3 at −11.76 ppm. This chemical shift differs by 1.37 ppm from that of the solvate cluster (Figure 3). The IR and NMR features, together with the decrease in the relative intensity of signal 3 in the presence of additional $CN^-$, demonstrates that the initial product is a cluster of $C_s$ symmetry. The occurrence of eight resonances, including signal 3, in the 2.0 and 3.0 equiv systems is exactly the number expected for a mixture of the six product clusters **5** (L = $CN^-$) and **20**–**24**. This result indicates that the initial product is not the cyanide analogue of fluxional **6**/**7** but is the Mo-ligated cluster **5**. In the 2.0 and 3.0 equiv cases clusters with different extents of further substitution are recognizable, i.e., **20**/**21** and **22**/**23**. However, the s and u isomers of each pair, while clearly present, cannot be distinguished because of the overlap of certain signals and the statistical weights of the isomers. The 4.0 equiv reaction product exhibits an absorption spectrum with $\lambda_{max}$ = 306 ($\epsilon_M$ 16 400) and 464 (5470) nm, the single symmetrical resonance 5 at −10.74 ppm, and $\nu_{CN}$ = 2120, 2095, 2020, and 1989 (w) $cm^{-1}$. None of the latter features arises from unbound cyanide, for which $\nu_{CN}$ = 2058 $cm^{-1}$ in acetonitrile. These results are entirely consistent with formation of the fully substituted cluster **24**, $[MoFe_3S_4(CN)_4(al_2cat)]^{3-}$, the first example of a $MoFe_3S_4$ (or $Fe_4S_4$) cluster with Fe–CN ligation. Previously we have reported two examples of the Mo–CN clusters **3**.[8]

**(f) At Mo Sites.** In order to determine the relative affinities of the ligands $RS^-$, $PEt_3$, and $CN^-$ for binding at the Mo site, a series of experiments with ~10 mM $[MoFe_3S_4(SPh)_3(al_2cat)(MeCN)]^{2-}$ (**2**), obtained from **1** (R = Ph)[6] by reaction 1 in acetonitrile, was carried out. This cluster, rather than **4**, was employed in order to suppress any Fe-site substitution, thereby promoting clean formation of the clusters **3** (here abbreviated as Mo–L) by reaction 2. This reaction was monitored by means of the intensities of *m′* resonances of Mo–L at −17.41 (L = $PhS^-$), −17.62 (L = $CN^-$), and −18.85 (L = $PEt_3$) ppm. In all cases formation of the initial Mo–L species from **2** and 1.0–1.1 equiv of $L^{0,1-}$ was quantitative. Reaction of Mo–SPh with 1.08 equiv of $PEt_3$ afforded the product ratio $Mo{-}PEt_3/Mo{-}SPh \cong 13{:}1$. Within Mo–SPh and 0.54 equiv of $PEt_3$ this ratio is 1.1:1. These observations are consistent with the failure of 1 equiv of $R_FS^-$ to displace phosphine from cluster **19** (L′ = $R_FS^-$; Figure 8). Treatment of $Mo{-}PEt_3$ with 1.06 equiv of $CN^-$ resulted in $Mo{-}CN/Mo{-}PEt_3$ = 3.2:1. When equilibrium was approached from the opposite side, by reaction of Mo–CN with 1.07 equiv of $PEt_3$, the product ratio is 3.4:1. In the system $Mo{-}PEt_3$ + 0.53 equiv of $CN^-$, this ratio is 0.80. These results establish the order of binding affinity to be $PhS^- < PEt_3 < CN^-$ in the clusters **3**.

## Summary

The following are the principal findings and conclusions of this investigation.

(1) The single-cubanes **2**, as $MoFe_3S_4$ double cubanes[3] and $Fe_nS_n$ clusters[23,24] (*n* = 2, 4), undergo complete thiolate ligand substitution with a stoichiometric amount of acetyl chloride (reaction 3) affording the $[MoFe_3S_4Cl_3(al_2cat)(solv)]^{2-}$ species **4**, isolated here as the THF solvate.

(2) $(Et_4N)_2[MoFe_3S_4Cl_3(al_2cat)(THF)]$ crystallizes in space group *C*2/*c* with imposed $C_s$ cluster symmetry, which requires two types of Fe sites, 2*m″* + *m′*. Dimensions of the $[MoFe_3S_4]^{3+}$ core are similar to those of cubanes of the same oxidation level. Comparison with $[MoFe_3S_4(S\text{-}p\text{-}C_6H_4Cl)_4(al_2cat)]^{3-}$ (**3**), the only other structurally defined single cubane,[4,8] indicates that the small differences in several cluster bond lengths arise from coordination of hard (**4**) vs. soft, electron-rich (**3**) ligands to the Mo atom. Proof of Mo–THF ligation in **4** supplements spectroscopic data in providing persuasive evidence for the existence in solution of the solvated clusters **2**,[2,6,8] which have not been isolated.

(3) Clusters exhibit isotropically shifted $^1H$ and $^{19}F$ NMR signals whose chemical shifts are sensitive to the extent of substitution and, with nonlabile Mo–L binding, to cluster symmetry, thereby permitting resolution of ligands at *m′* and *m″* sites and detection and differentiation of all product clusters. Rapid exchange of Mo–solv ligands with bulk solvent results in fluxional clusters whose *m′* and *m″* sites are equilibrated by a process proposed to be that in Figure 4. The sensitivity of $^{19}F$ isotropic shifts to structures of Mo–Fe–S and Fe–S clusters has been further demonstrated elsewhere.[7,21]

(4) The following ligand substitution patterns have been established for the solvate clusters **4** at ~10 mM by NMR spectroscopy.

(a) In acetonitrile and $Me_2SO$ solutions 1–3 equiv of thiolate ($PhS^-$, $R_FS^-$) react exclusively or predominantly *at Fe sites* to yield the substituted clusters **6**–**9** and **2**. Members of the pairs **6**/**7** and **8**/**9** could not be detected owing to cluster fluxionality. The absence of this behavior in Mo–SR clusters permitted detection of a small minority population of the isomers **11** and **12** in the **4**/$R_FS^-$ system in acetonitrile. Clusters **13** and **14** were not observed.

---

[37] Infrared measurements were performed on $CH_3CN$ solutions containing initially 32 mM **4**.

(b) In acetonitrile and $Me_2SO$ solutions 1 equiv of $PEt_3$ reacts exclusively *at the Mo site* to yield **5** (L = $PEt_3$), which does not react further with 2 equiv of the phosphine. In acetonitrile solution 1 equiv of $CN^-$ forms predominantly *Mo-ligated* **5** (L = $CN^-$). This species reacts with additional equivalent of $CN^-$ to afford all possible substituted clusters **20–24**, which are stereochemically rigid.

(c) Cluster **5** (L = $PEt_3$) in acetonitrile solution with 1–3 equiv of $R_FS^-$ forms all possible substituted clusters **15–19**, which are nonfluxional. A fourth equivalent of thiolate does not displace bound phosphine.

(d) Product cluster ratios in the systems **4** and **5** (L = $PEt_3$) + 1 or 2 equiv of $R_FS^-$ approach statistical values assuming three equivalent Fe sites (Table IV). For example, the following observed (statistical) values apply to both **4** and **5** + 1 equiv of $R_FS^-$ in acetonitrile: [2,1]/[1,2] = 2.0 (2), [2,1]/[0,3] = 13 (12), [1,2]/[0,3] = 6.4 (6). Deviations of **4**/$R_FS^-$ in $Me_2SO$ from statistical distributions are more pronounced. For the systems **5** + 1 or 2 equiv of $R_FS^-$ large departures from the statistical isomer ratio u/s = 2 are observed for [2,1] (**15**,**16**) and [1,2] (**17**,**18**) clusters. These ratios, **16**/**15** = 9.5 and **18**/**17** = 0.52, demonstrate discrimination against binding at the *m′* site. This situation is a likely consequence of two factors: the shorter and presumably stronger Fe–Cl bond at this site (structural feature iv) and steric interactions between the bulky phosphine and thiolate which are more destabilizing than if the latter were located at a *m″* site.

(e) From the results of this and another investigation[6] relative binding affinities at the Mo site in the clusters **2** are MeCN < $Me_2SO$ ~ DMF and in clusters **3** in acetonitrile $RS^-$ < $PEt_3$ < $CN^-$. In this solvent 1 equiv of each ligand reacts quantitatively with **2** to form nonfluxional **3**. A number of other ligands such as $N_3^-$, pyridine, and piperidine form labile, fluxional clusters; these systems are currently under study.[38] Carbon monoxide does not react with $[MoFe_3S_4(SR)_3(al_2cat)(MeCN)]^{2-}$. It does react irreversibly with the reduced cluster with R = p-$C_6H_4Cl$. A number of products are formed, one which has been tentatively identified as the mono-CO adduct.[8]

This investigation provides the first information on the reactivity properties of substitutionally labile Mo and Fe atoms in a common cluster, $[MoFe_3S_4Cl_3(al_2cat)(solv)]^{2-}$ (**4**), having the same spin state ($S = {}^3/_2$)[7,10] as, and coordination sites resembling those in, the FeMo proteins and FeMo-co of nitrogenase. Highly preferential binding of thiolate at the Fe sites of the synthetic cluster finds an *apparent* parallel in the reaction of FeMo-co with 1 equiv of $R_FS^-$ and p-$FC_6H_4S^-$ in *N*-methylformamide solution at ambient temperature. Here binding has been deduced to occur at a Fe site on the basis of the isotropically shifted $^{19}F$ resonances of the resultant complexes.[7] A distinct difference between FeMo-co and the synthetic clusters is that the former appears to bind only one ligand even in the presence of excess thiolate. Further parallel reactivity would suggest Mo-site binding by phosphines and limited cyanide, reactions potentially detectable by monitoring of $^{19}F$ shifts of bound thiolate. These and related reactions offer possible means of derivatizing FeMo-co in a form that might prove more susceptible to crystallization than is the native cluster itself. Lastly, the present results constitute the most comprehensive study of relative reactivities of metal sites in a heteronuclear cluster. The approach described here is being extended to the reactions of oxidized and reduced solvated clusters with the same and other ligands, including N-coordinating ligands and potentially reducible substrates. Because of the paramagnetism ($S = 2$) of the $[MoFe_3S_4]^{2+}$ core of reduced clusters, large isotropic shifts are observed[5,8] and, on the basis of the spectrum of one phosphine-ligated cluster,[8] *m′* and *m″* sites are well-resolved in nonfluxional species.

**Acknowledgment.** This research was supported by NSF Grant 81-06017. X-ray and NMR equipment used in this research was obtained by NSF Grants CHE 80-00670 and CHE 80-08891. We thank J. M. Berg for cluster volume calculations and Dr. P. K. Mascharak for experimental assistance.

**Registry No. 1** (R = Et)·4($Et_4N$), 82281-65-0; **1** (R = Ph), 82196-50-7; **2** (L = $Me_2SO$; R = Ph), 85749-41-3; **2** (L = MeCN; R = Ph), 85749-44-6; **2** (L = $Me_2SO$; R = p-$C_6H_4CF_3$), 85749-48-0; **2** (L = MeCN; R = p-$C_6H_4CF_3$), 85749-54-8; **2** (L = $CN^-$; R = Ph), 85749-60-6; **2** (L = $PEt_3$; R = Ph), 85749-61-7; **4** (solvent = THF)·2($Et_4N$), 85749-35-5; **4** (solvent = MeCN), 85749-36-6; **4** (solvent = $Me_2SO$), 85749-37-7; **5** (L = $PEt_3$), 85749-38-8; **5** (L = $CN^-$), 85749-56-0; **6/7** (L = $Me_2SO$; R = Ph), 85749-39-9; **6/7** (L = MeCN; R = Ph), 85749-42-4; **6/7** (L = $Me_2SO$; R = p-$C_6H_4CF_3$), 85749-46-8; **6/7** (L = MeCN; R = p-$C_6H_4CF_3$), 85749-52-6; **8/9** (L = $Me_3SO$; R = Ph), 85749-40-2; **8/9** (L = MeCN; R = Ph), 85749-43-5; **8/9** (L = $Me_2SO$, R = p-$C_6H_4CF_3$), 85749-47-9; **8/9** (L = MeCN; R = p-$C_6H_4CF_3$), 85749-53-7; **10** (L = $PhS^-$; R = Ph), 85749-45-7; **10** (L = $CF_3C_6H_4$-p-$S^-$; R = p-$C_1H_4CF_3$), 84934-99-6; **11** (L = $F_3CC_6H_4$-p-$S^-$; R = p-$C_6H_4CF_3$), 85749-55-9; **12** (L = $F_3CC_6H_4$-p-$S^-$; R = p-$C_6H_4CF_3$), 85848-59-5; **15** (L = $PEt_3$; L′ = $F_3CC_6H_4$-p-$S^-$), 85749-49-1; **16** (L = $PEt_3$; L′ = $F_3CC_6H_4$-p-$S^-$), 85798-61-4; **17** (L = $PEt_3$; L′ = $F_3CC_6H_4$-p-$S^-$), 85749-50-4; **18** (L = $PEt_3$; L′ $F_3CC_6H_4$-p-$S^-$), 85798-62-5; **19** (L = $PEt_3$; L′ = $F_3CC_6H_4$-p-$S^-$), 85749-51-5; **20/21**, 85749-57-1; **22/23**, 85749-58-2; **24**, 85749-59-3.

**Supplementary Material Available:** X-ray structural data for $(Et_4N)_2[MoFe_3S_4Cl_3(al_2cat)(THF)]$—tables of thermal parameters, positional parameters of the cations, calculated hydrogen atom coordinates, and values of $10|F_o|$ and $10|F_c|$ (20 pages). Ordering information is given on any current masthead page.

---

(38) Singh, R.; Holm, R. H., results to be published.